

Entanglement Stabilization using Parity Detection and Real-Time Feedback in Superconducting Circuits

Science Team: C. Andersen, S. Balasius, J.-C. Besse, M. Collodo, J. Heinsoo, J. Herrmann, S. Krinner, P. Kurpiers, P. Magnard, G. Norris, A. Remm, P. Scarlino, T. Walter, C. Eichler, A. Wallraff *(ETH Zurich)*
B. Royer, and A. Blais *(Université de Sherbrooke)*

Technical Team: A. Akin, M. Frey, M. Gabureac, J. Luetolf



SWISS NATIONAL SCIENCE FOUNDATION



Acknowledgements

Former group members now Faculty/PostDoc/PhD/Industry

A. Abdumalikov (Gorba AG)
 M. Allan (Leiden)
 M. Baur (ABB)
 J. Basset (U. Paris Sud)
 S. Berger (AWK Group)
 R. Bianchetti (ABB)
 D. Bozyigit (MIT)
 A. Fedorov (UQ Brisbane)
 A. Fragner (Yale)
 S. Filipp (IBM Zurich)
 J. Fink (IST Austria)
 T. Frey (Bosch)
 S. Garcia (College de France)
 S. Gasparinetti (Chalmers)
 M. Goppl (Sensirion)
 J. Govenius (Aalto)
 L. Huthmacher (Cambridge)
 D.-D. Jarausch (Cambridge)

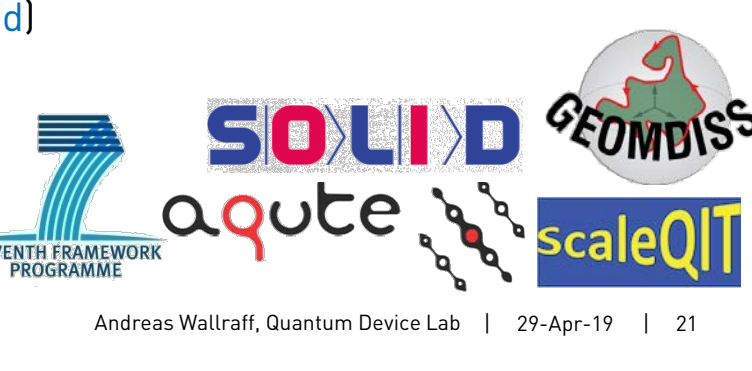
K. Juliusson (CEA Saclay)
 C. Lang (Radiornor)
 P. Leek (Oxford)
 P. Maurer (Chicago)
 J. Mlynek (Siemens)
 M. Mondal (IACS Kolkata)
 M. Oppliger
 M. Pechal (Stanford)
 A. Potocnik (imec),
 G. Puebla (IBM Zurich)
 A. Safavi-Naeini (Stanford)
 Y. Salathe (Zurich Inst.)
 M. Stammeier (Huba Control)
 L. Steffen (AWK Group)
 A. Stockklauser (Rigetti)
 T. Thiele (UC Boulder, JILA)
 A. van Loo (Oxford)
 D. van Woerkom (Microsoft)
 S. Zeytinoğlu (ETH Zurich)

Collaborations (last 5 years) with groups of

A. Bachtold (ICFO Barcelona)
 A. Blais (Sherbrooke)
 A. Chin (Cambridge)
 M. Delgado (UC Madrid)
 L. DiCarlo (TU Delft)
 P. Domokos (WRC Budapest)
 K. Ensslin (ETH Zurich)
 J. Faist (ETH Zurich)
 A. Fedorov (Brisbane)
 K. Hammerer (Hannover)
 M. Hartmann (Hariot Watt)
 T. Ihn (ETH Zurich)
 F. Merkt (ETH Zurich)
 L. Novotny (ETH Zurich)
 M. A. Martin-Delgado (Madrid)
 T. J. Osborne (Hannover)
 S. Schmidt (ETH Zurich)
 C. Schoenenberger (Basel)

www.qudev.ethz.ch

E. Solano (UPV/EHU)
 H. Tureci (Princeton)
 W. Wegscheider (ETH Zurich)



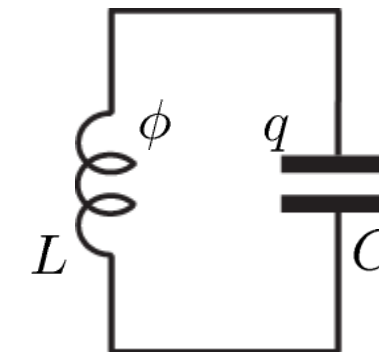
Superconducting Circuits as Components for a Quantum Computer

constructing quantum electronic circuits from basic circuit elements:



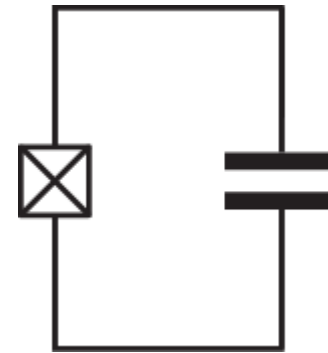
Josephson junction:
a non-dissipative
nonlinear element
(inductor)

harmonic LC oscillator:



$$H = \hbar\omega(\hat{a}^\dagger\hat{a} + \frac{1}{2})$$

anharmonic oscillator:

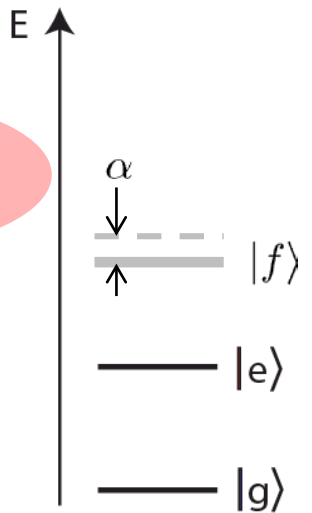


$$H \approx \hbar(\omega_{ge}\hat{b}^\dagger\hat{b} - \frac{\alpha}{2}\hat{b}^{\dagger 2}\hat{b}^2)$$

electronic photon



electronic artificial atom



A Single Architecture ...

... for fast, high fidelity single shot readout

F ~ 98.25 (99.2) % at 48 (88) ns integration time and resonator population n ~ 2.2 with

- Optimized sample design
- Low-noise phase-sensitive Josephson parametric amplifier

T. Walter, P. Kurpiers *et al.*, *Phys. Rev. Applied* 7, 054020 (2017)

... for unconditional reset

- 99% reset fidelity in < 300 ns

P. Magnard *et al.*, *Phys. Rev. Lett.* 121, 060502 (2018)

... that is multiplexable

- Single feedline for 8 qubits (nodes)
- Reduced cross-talk using Purcell filters

J. Heinsoo *et al.*, *Phys. Rev. Applied* 10, 034040 (2018)

... for parity check with feedback and reset

C. Andersen, A. Remm, S. Balasius *et al.*, *arXiv:1902.06946* (2019)

... for remote entanglement and state transfer, with time-bin encoding against photon loss

- Deterministic, 50 kHz rate
- ~ 80% transfer and entanglement fidelity

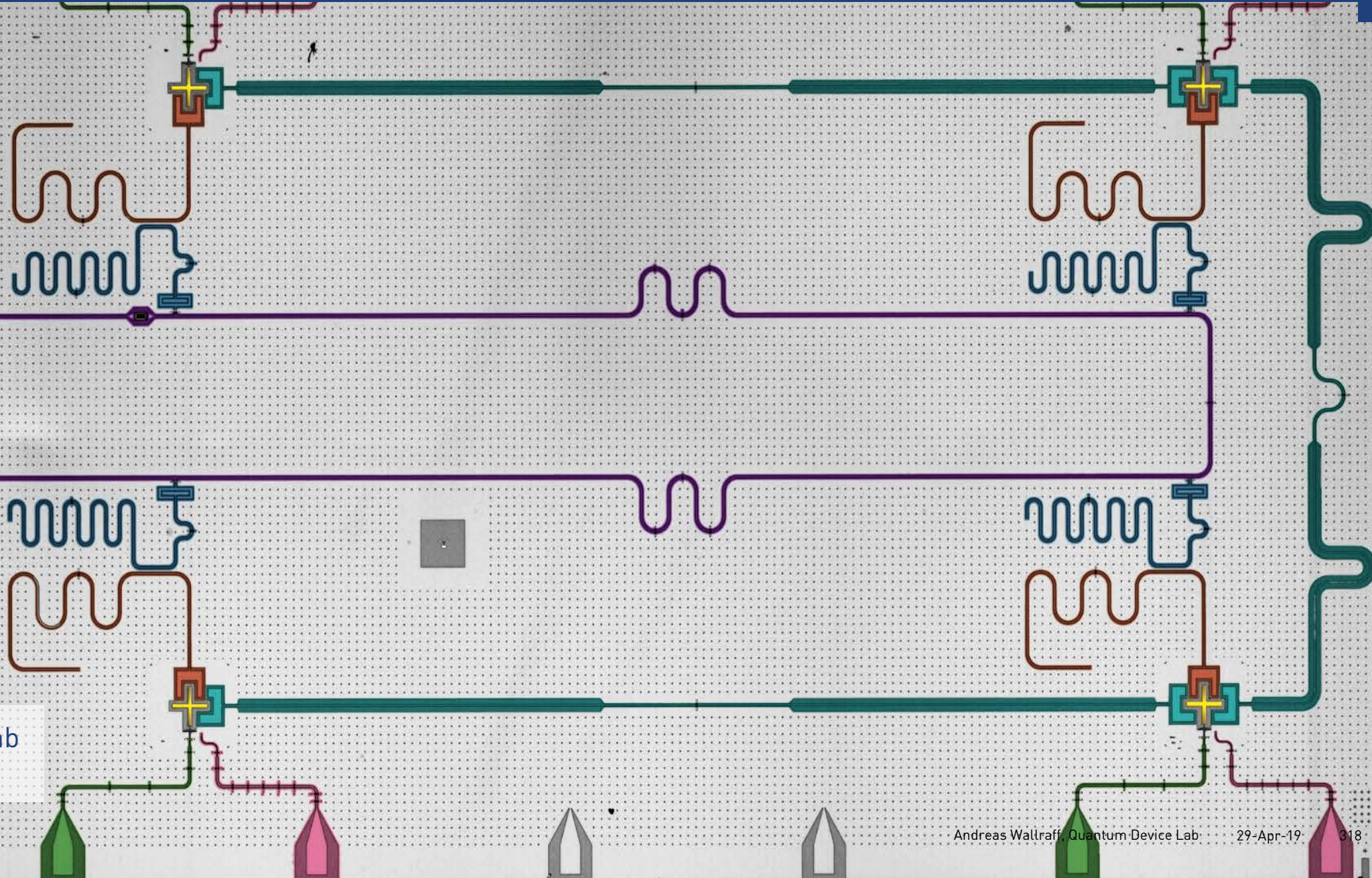
P. Kurpiers, P. Magnard *et al.*, *Nature* 558, 264 (2018)

P. Kurpiers, M. Pechal *et al.*, *arXiv:1811.07604* (2018)

... for QND single-shot single photon detection

- 71% internal detection fidelity
 - 13% dark count probability
 - 16% detection inefficiency

J.-C. Besse *et al.*, *Phys. Rev. X* 8, 021003 (2018)



Quantum Device Lab
ETH Zurich (2018)

Parity Reset and Correction

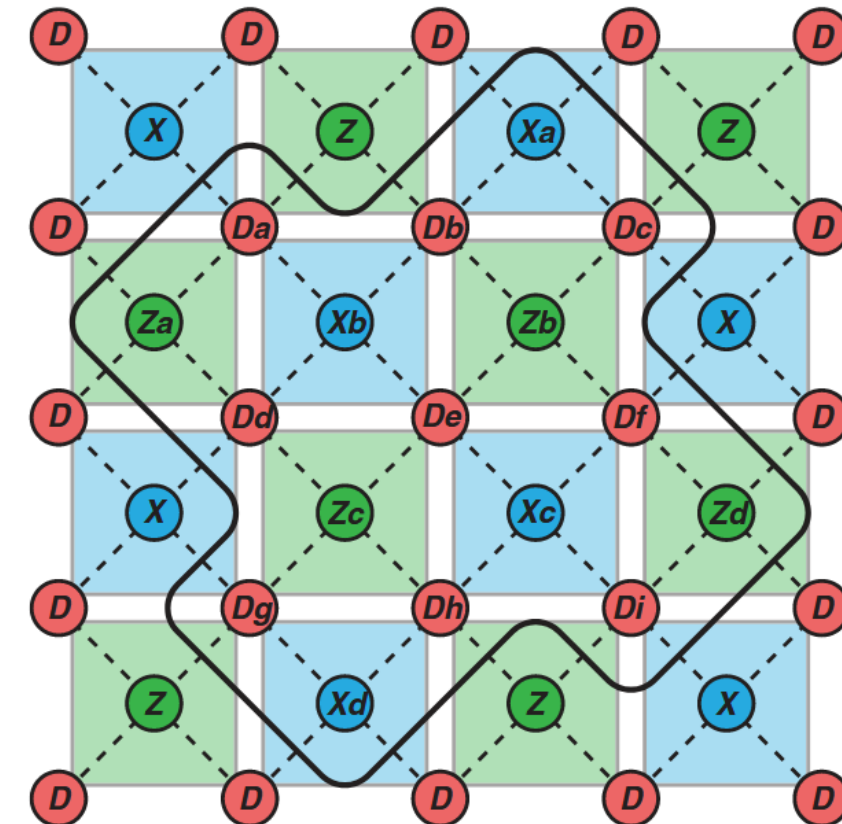
Quantum error correction

- Encode quantum information in multiple qubits
- Measure multi-qubit stabilizers
- Correct errors based on stabilizer measurements

Surface code

- Stabilizers are weight-4 XXXX- and ZZZZ-parity measurements
- At edge of surface: weight-2 XX- and ZZ- parity measurements

Demonstrating parity measurements and feedback is a step towards realizing quantum error correction.



Versluis *et al.*, Phys. Rev. Applied 8, 034021 (2017)

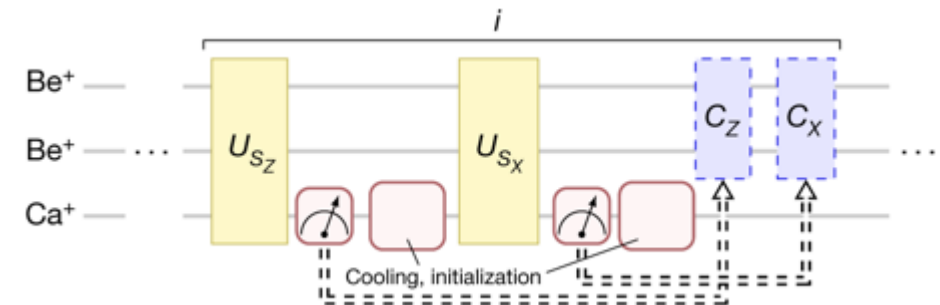
Parity Reset and Correction: Prior Work

With superconducting circuits:

- Bit-flip code with weight-2 parity checks
Riste et al, *Nat Comm* 6, 6983 (2015)
Kelly et al, *Nature* 519, 66–69 (2015)
- Simultaneous XX and ZZ checks
Corcoles et al, *Nat Comm* 6, 6979 (2015)
- Weight-4 parity check
Takita et al, *PRL* 117, 210505 (2016)
- Feedback with superconducting qubits
Steffen et al, *Nature* 500, 319–322 (2013)
Riste et al, *Nature* 502, 350–354 (2013)

With trapped ions:

- 50 repetitions of interleaved XX and ZZ detection and feedback for Bell state stabilization
Negnevitsky et al., *Nature* 563, 527–531 (2018)



Goal for superconducting qubits:

- Repeated parity correction in a multi-qubit architecture using feedback
- Demonstration of a general programmable feedback architecture

Parity Measurements and Quantum Error Correction

Parity of 2-qubit Bell states

(a)

Map to even (+1) XX subspace
D2: R_z^π

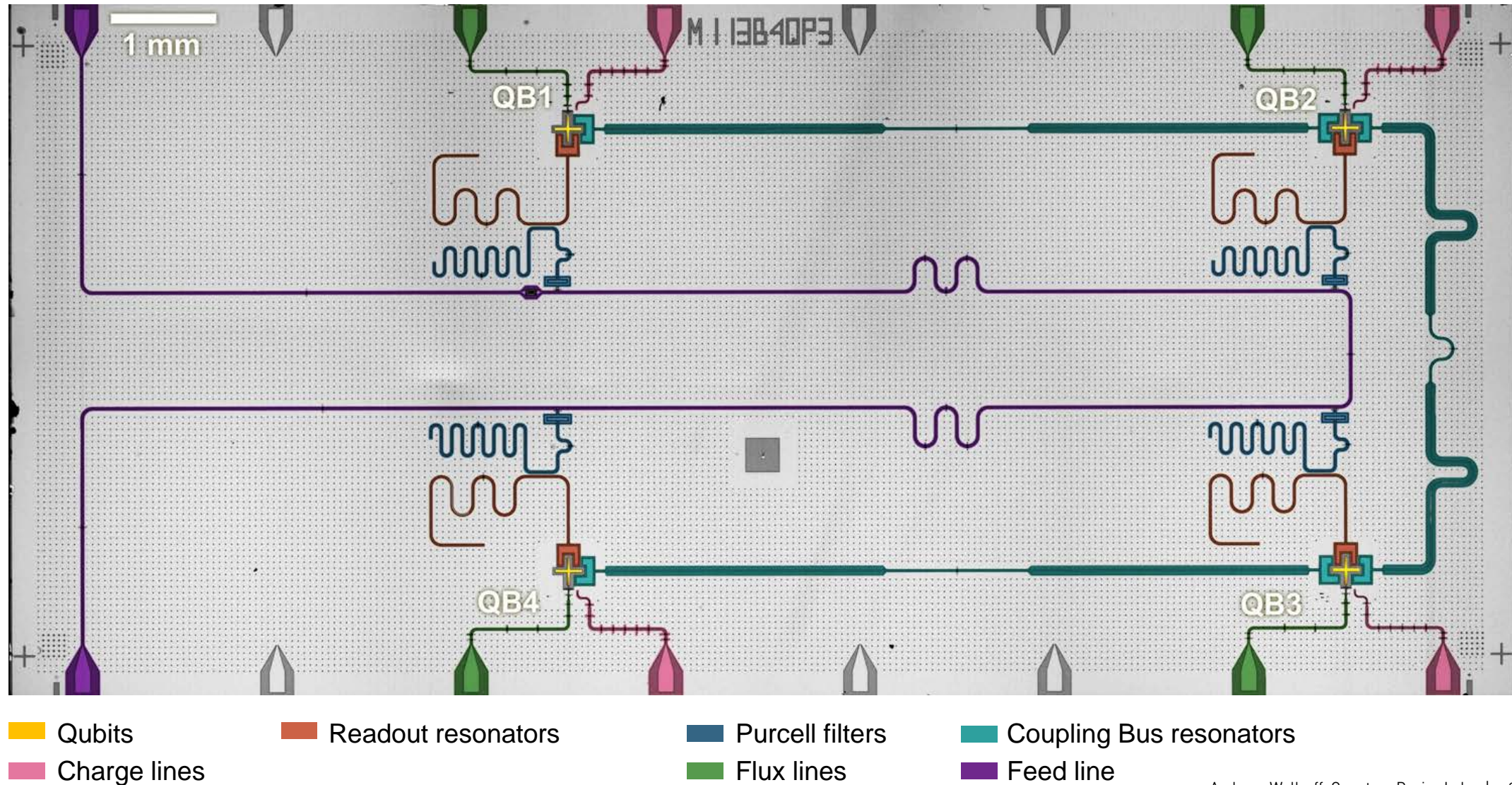
XX		
ZZ	+1	-1
+1	$ \Phi^+\rangle = \frac{ 00\rangle + 11\rangle}{\sqrt{2}}$	$ \Phi^-\rangle = \frac{ 00\rangle - 11\rangle}{\sqrt{2}}$
-1	$ \Psi^+\rangle = \frac{ 01\rangle + 10\rangle}{\sqrt{2}}$	$ \Psi^-\rangle = \frac{ 01\rangle - 10\rangle}{\sqrt{2}}$

Map to even (+1)
ZZ subspace
D2: R_x^π

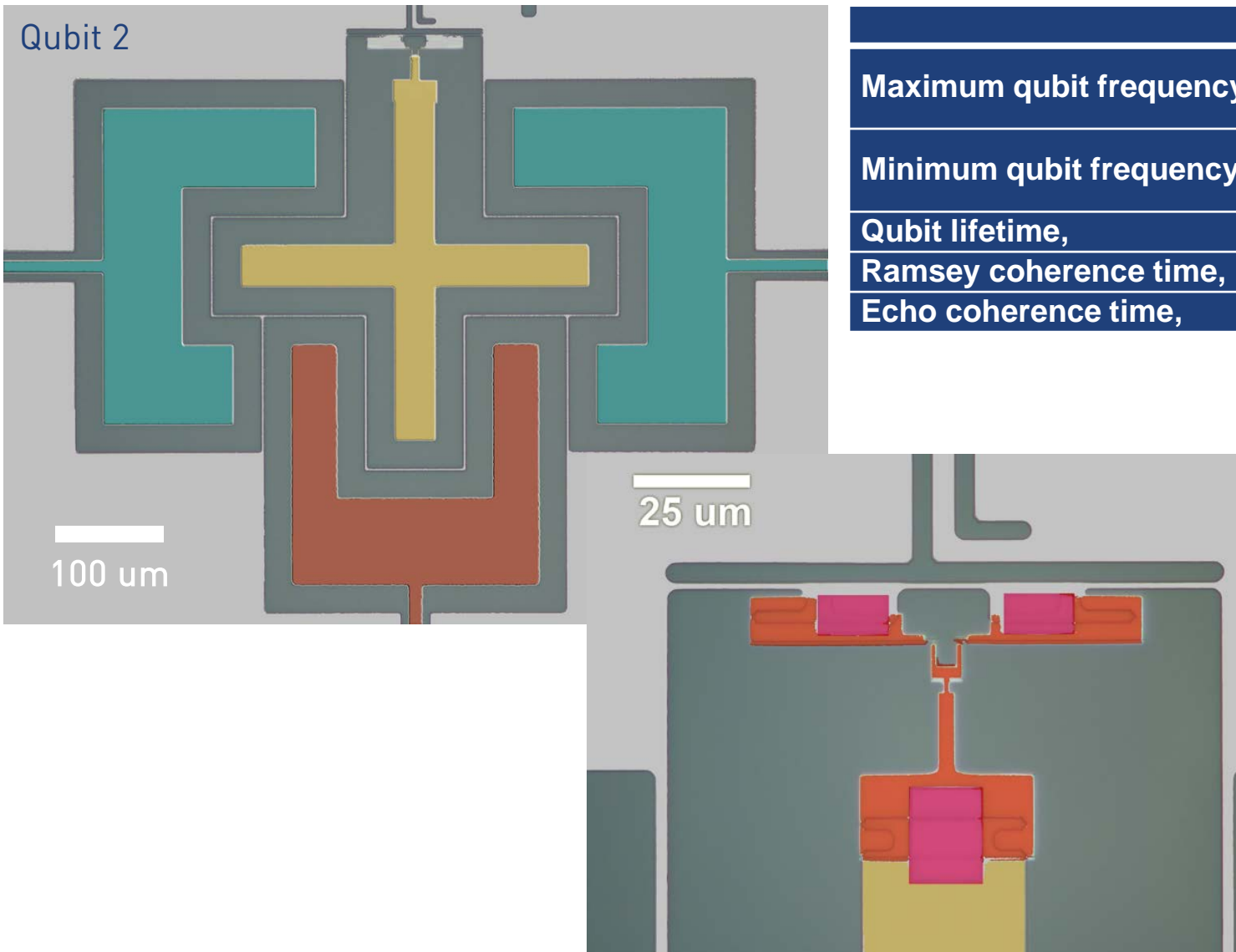
- Measure parity using ancilla qubit
- Stabilize selected parity sub-space
 - here $ZZ = +1$ and $XX = +1$
 - resulting in Φ^+

- Single-qubit Pauli operators X , Y and Z do not commute $[X, Z] = 2iY$
- Two-qubit parity operators X_1X_2 and Z_1Z_2 commute $[X_1X_2, Z_1Z_2] = 0$
 - XX and ZZ have a set of common eigenstates

4 Qubit Device with Improved Parameters



Qubit Design and Performance



		QB1	QB2	QB3	QB4
Maximum qubit frequency,	$\omega_{Q,\max}/2\pi$ (GHz)	5.721	5.210	5.530	5.160
Minimum qubit frequency,	$\omega_{Q,\min}/2\pi$ (GHz)	5.083		4.880	4.386
Qubit lifetime,	T_1 (μs)	19.7	10.3	23.6	43.1
Ramsey coherence time,	T_2^* (μs)	14.3	11.3	14.2	10.7
Echo coherence time,	T_2^e (μs)	19.3	12.1	19.5	20.2

- Coherence times are measured at the boldfaced frequencies
- Qubits have asymmetric SQUIDs (ratio 1:8) for decreased flux noise sensitivity

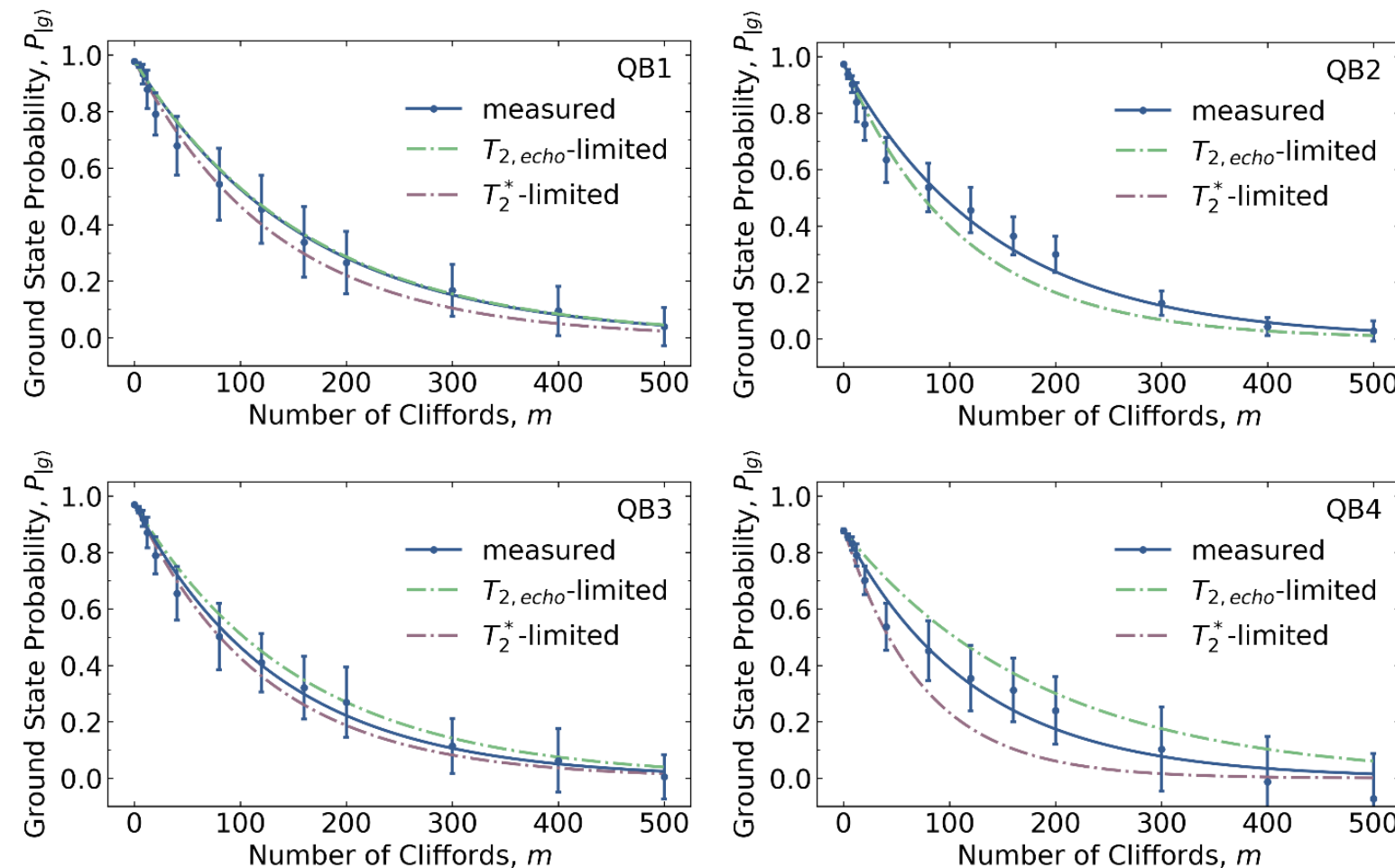
Single Qubit Gate Fidelity

Randomized benchmarking (RB)

- 50 ns DRAG pulses with 10 ns σ .
- Clifford decomposition in terms of X rotations and virtual Z gates.
- Gate error at T_1 limit, $r_{coh-lim}$.

Average Error per Clifford, r_{Cl}

	r_{Cl} (measured)	r_{Cl} simulated (T1, T2 errors)
QB1	$0.31\% \pm 0.07\%$	0.31%
QB2	$0.35\% \pm 0.05\%$	0.40%
QB3	$0.37\% \pm 0.08\%$	0.32%
QB4	$0.40\% \pm 0.14\%$	0.27%



Epstein *et al.*, Phys. Rev. A 89, 062321 (2014)

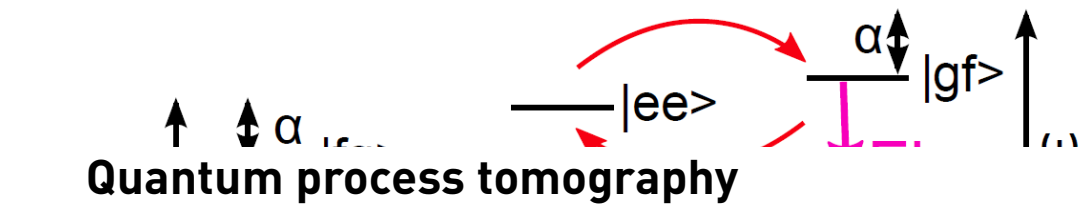
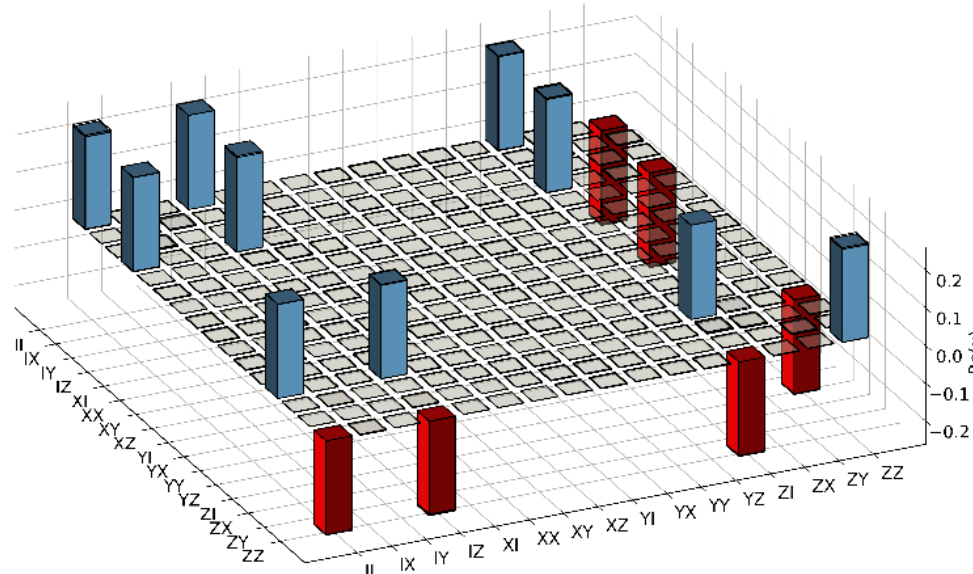
McKay *et al.*, Phys. Rev. A 96, 022330 (2017)

Two Qubit Gate Fidelity

C-PHASE gate ($|ee\rangle$, $|gf\rangle$)

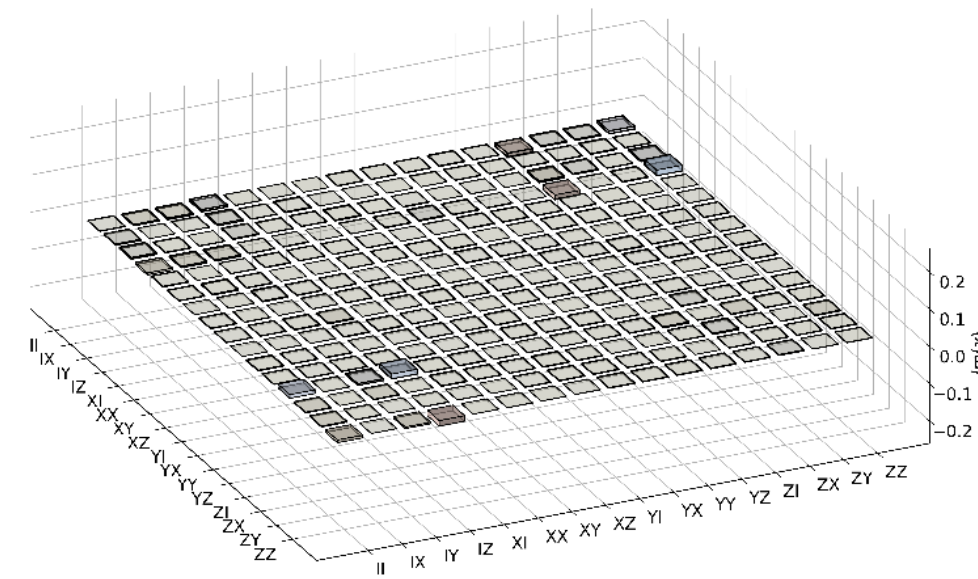
- 100 ns square flux pulse with 40 ns buffers
- Finite (FIR) and infinite impulse response (IIR) filters

QB1-QB2 QB2-QB3



- χ matrices for average gate fidelity
- Simulation with measured coherence times

	measured F	simulated F (T1, T2)
QB1-QB2	98.76%	99.17%
QB2-QB3	99.43%	99.5%



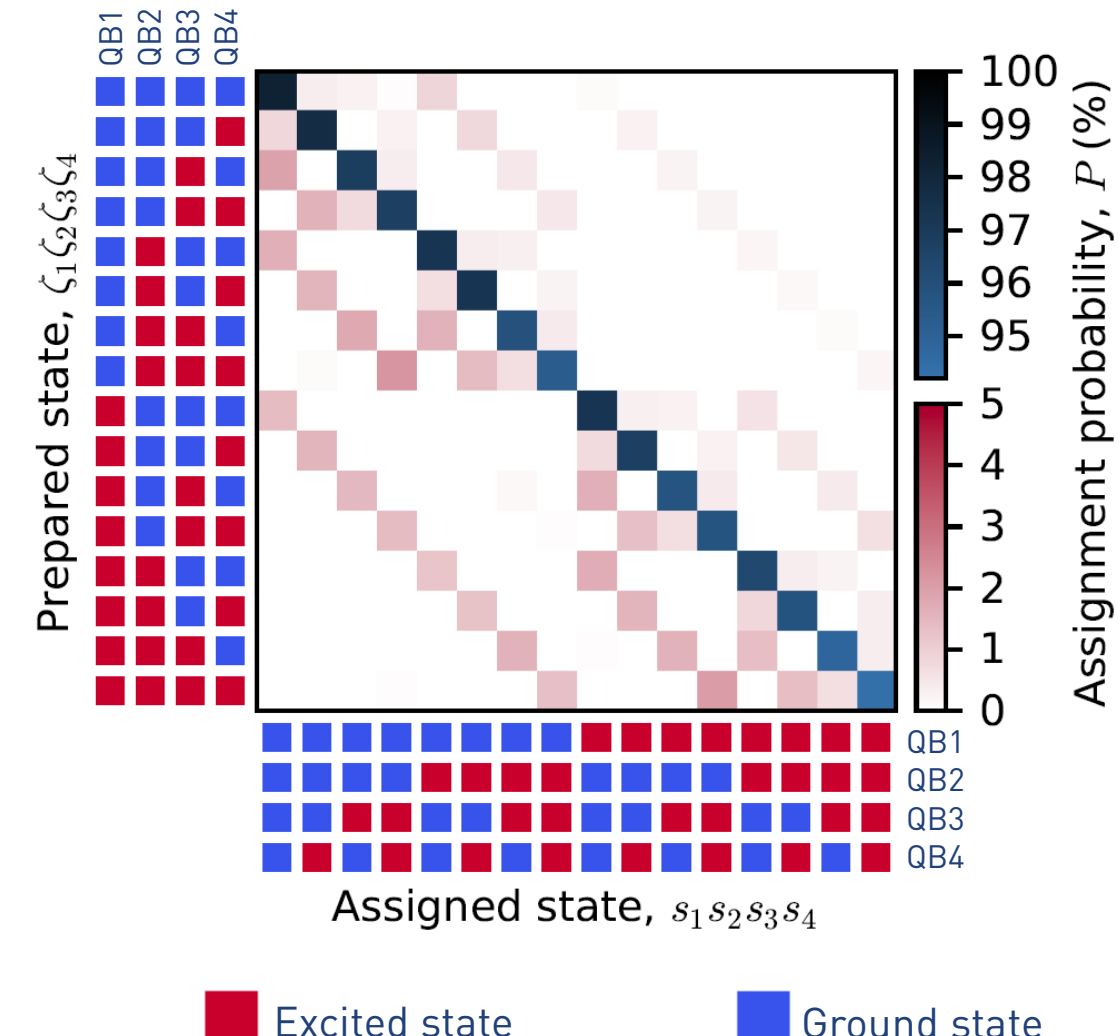
Multiplexed Readout

Readout parameters:

- Readout pulse length: 200 ns
- Integration time: 400 ns
- Detection efficiency: 25% - 35%
- Dispersive shift: 1.6 MHz – 3.9 MHz
- Effective readout linewidth: 1.5 MHz – 6.1 MHz

Readout Assignment Fidelities:

	QB1	QB2	QB3	QB4
Individual readout	99.23%	98.59%	99.05%	99.40%
Multiplexed readout, other qubits in $ g\rangle$	99.22%	98.72%	98.81%	99.32%
Multiplexed readout, avg. over other qubits prep. states	99.15%	98.72%	99.01%	99.38%

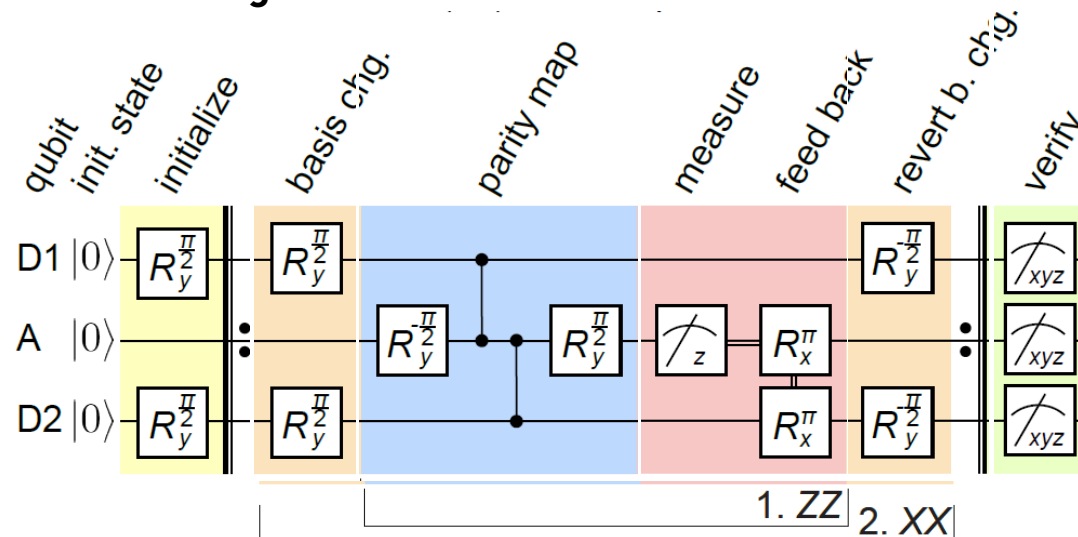


C. Andersen, A. Remm, S. Balasius et al., *arXiv:1902.06946* (2019)

Heinsoo *et al.*, *Phys. Rev. Applied* **10**, 034040 (2018).

Repeated Weight-2 ZZ- & XX-Parity Measurements

Circuit Diagram

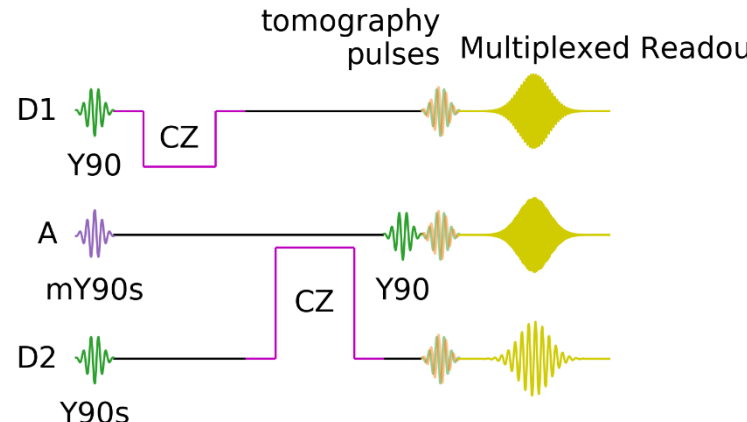


R_{xyz}^θ single qubit gate ---_{xyz} measurement $\parallel : \parallel$ n repetitions
 two-qubit gate —— feedback

- **$|++\rangle$ state preparation** of data qubits D1 and D2
- **ZZ parity measurements** with **coherent operations** between D1, D2 and ancilla qubit A followed by **readout** of A
- Subspace stabilization by **feedback** pulse conditioned on A measurement outcome
 - π pulse if $|e\rangle$
 - No pulse if $|g\rangle$
- **Active reset** of ancilla qubit
- **Verification**
- XX parity measurements with **basis changes**
- Repeated XX-ZZ protocol deterministically stabilizes the **Bell state**: $|00\rangle + |11\rangle$

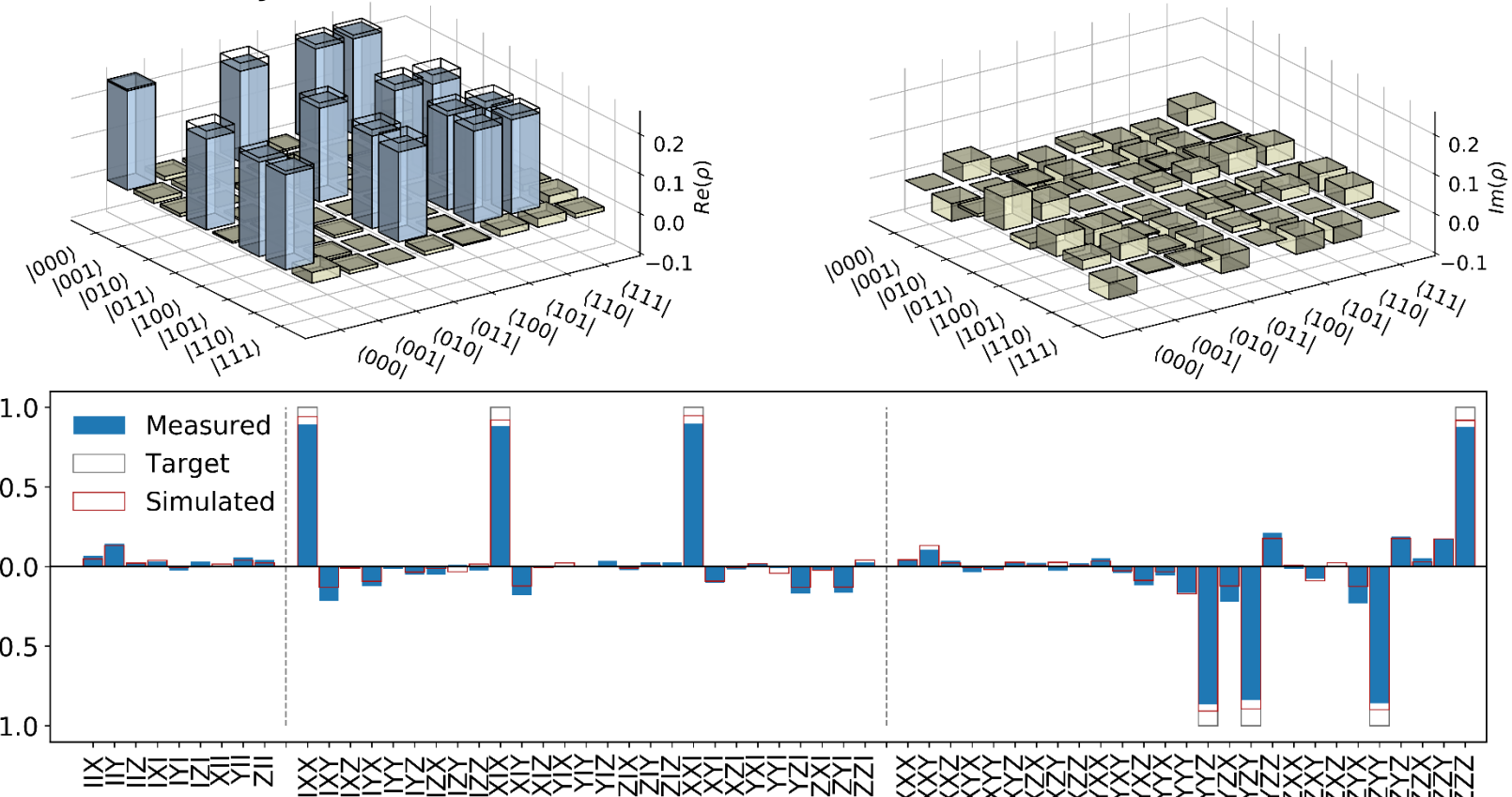
Coherent Dynamics of Weight-2 ZZ-Parity Measurement

Pulse sequence



- 50 ns **DРАG pulses**
- **CZ gates:**
 - 96 ns QB1-QB2
 - 105 ns QB2-QB3
 - 40 ns buffers
- 200 ns **R0 pulses**
 - 20 ns Gaussian filters

Measured density matrix and Pauli sets

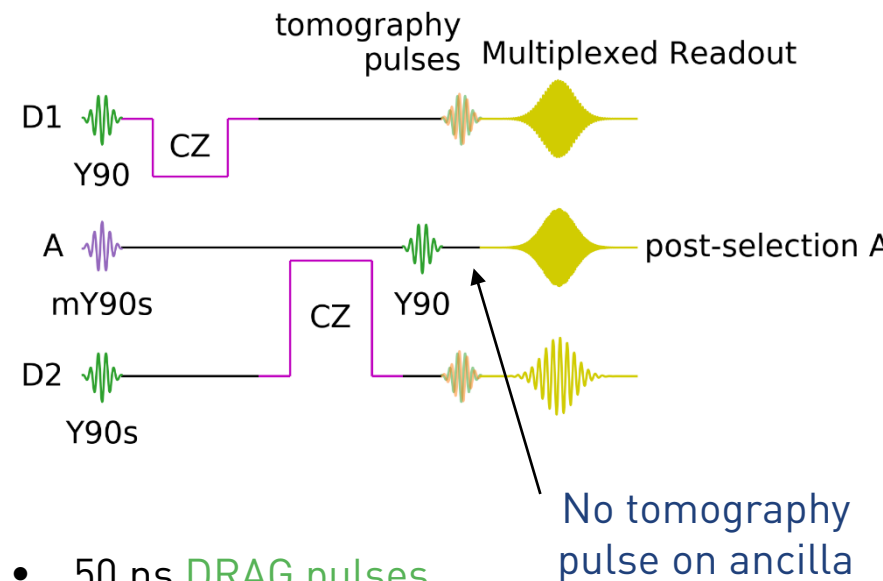


Fidelity:

- Experiment $F = 94.2\%$
- Simulation $F = 92.8\%$
- 97.6% overlap
- Compare to 3-qubit GHZ $F = 96.0\%$ in **Barends et al. *Nature* 508, 500 (2014)**

Weight-2 ZZ-Parity Measurements Post Selected on Ancilla Msrmnt

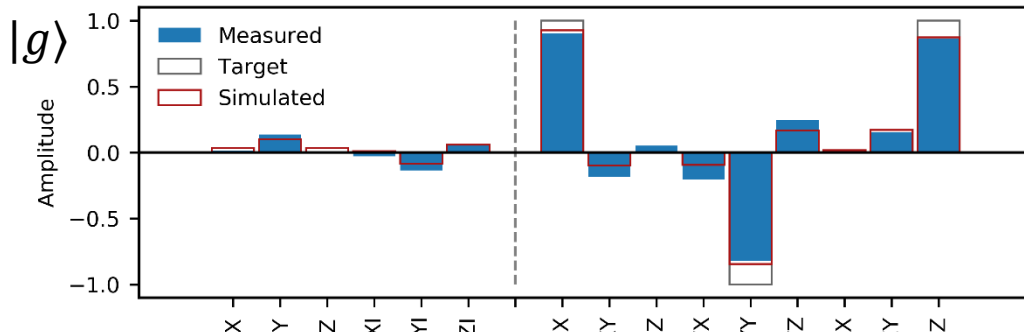
Pulse sequence



- 50 ns **DРАG pulses**
- **CZ gates:**
 - 96 ns QB1-QB2
 - 105 ns QB2-QB3
 - 40 ns buffers
- 200 ns **R0 pulses**
 - 20 ns Gaussian filters

Positive ZZ parity

Ancilla detected in $|g\rangle$

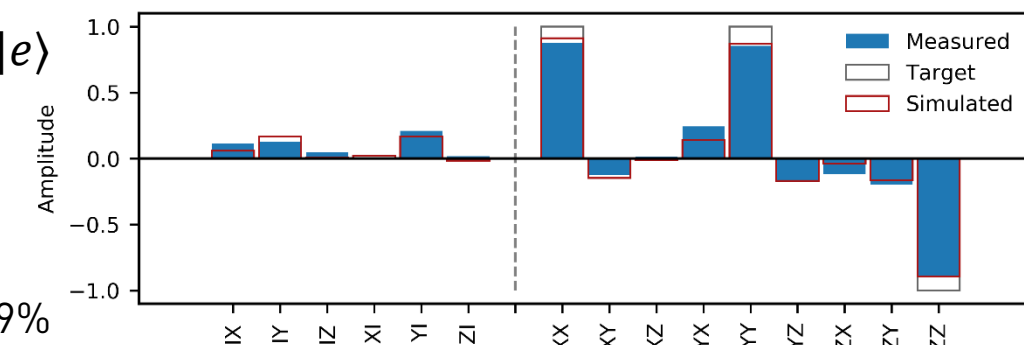


Fidelity

- Experiment F = 93.8%
- Simulation F = 91.1%

Negative ZZ parity

Ancilla detected in $|e\rangle$

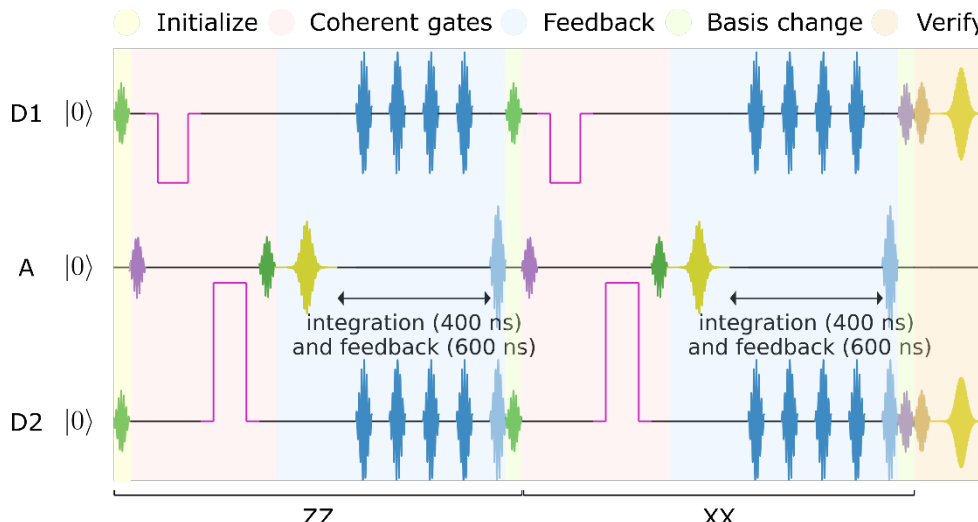


Fidelity

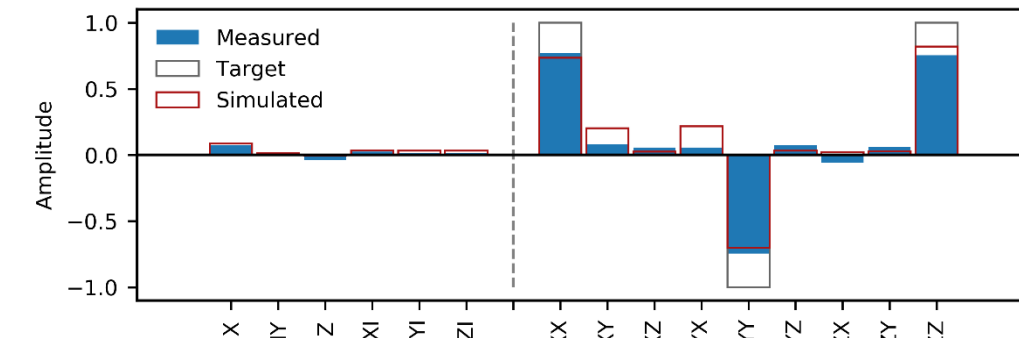
- Experiment F = 92.9%
- Simulation F = 91.9%

Weight-2 ZZ-, ZZ- & XX-Parity Measurements with Feedback

Pulse sequence



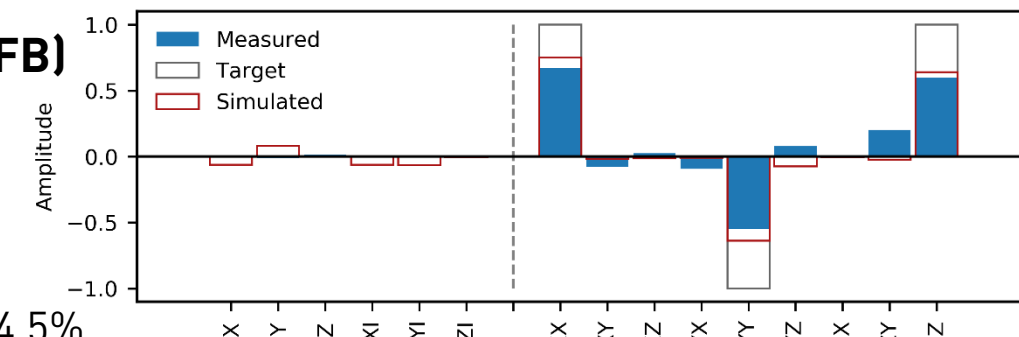
Positive ZZ parity stabilized (FB)



Fidelity

- Experiment F = 86.7%
- Simulation F = 81.4%
- Overlap F = 98.1%

Positive ZZ & XX parity stabilized (FB)

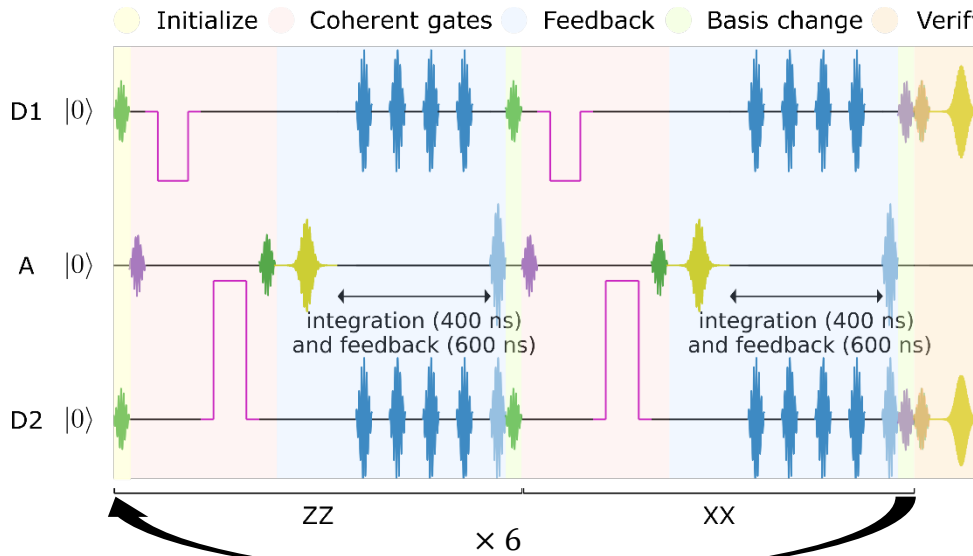


Fidelity

- Experiment F = 74.5%
- Simulation F = 75.6%
- Overlap F = 97.7%

Repeated (6x) Weight-2 ZZ & XX Parity Measurements with Feedback

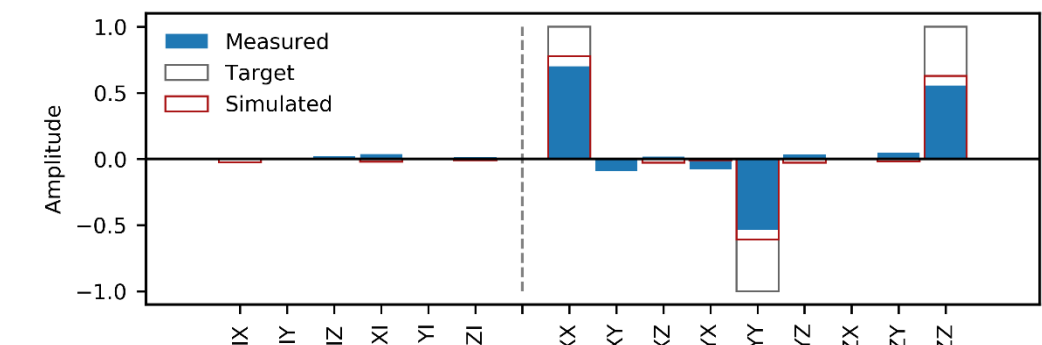
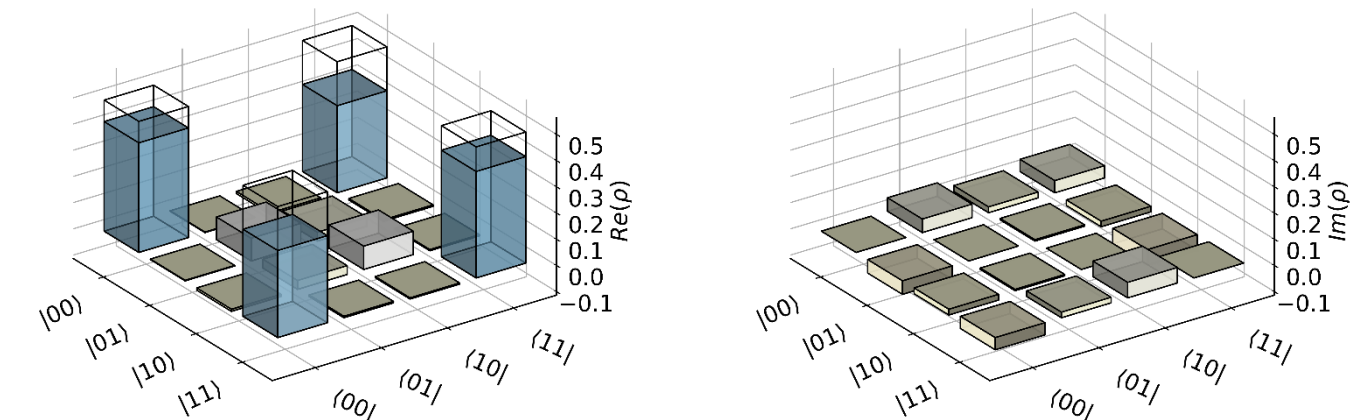
Pulse sequence



- Y90
- mY90
- CZ
- X180: DD Pulses
- X180: Reset & Correct
- Tomo. Pulses
- (M)RO

12 feedback rounds in total

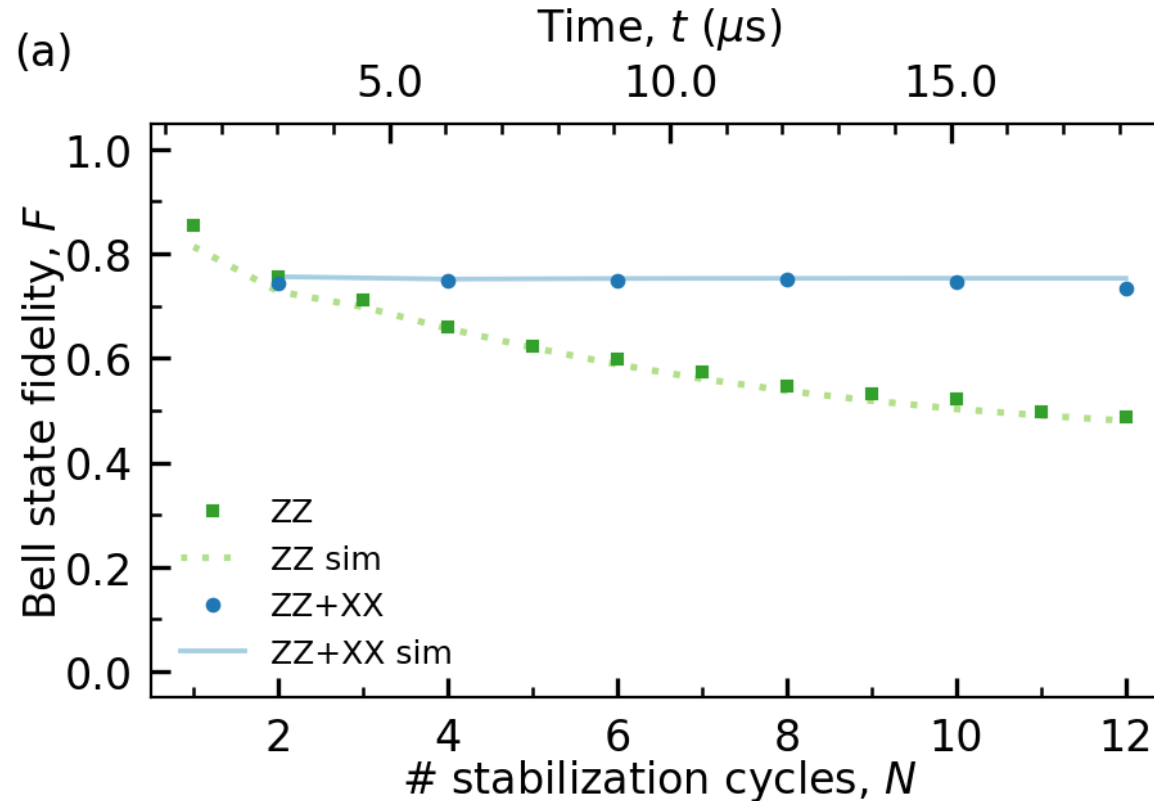
Measured density matrix and Pauli sets



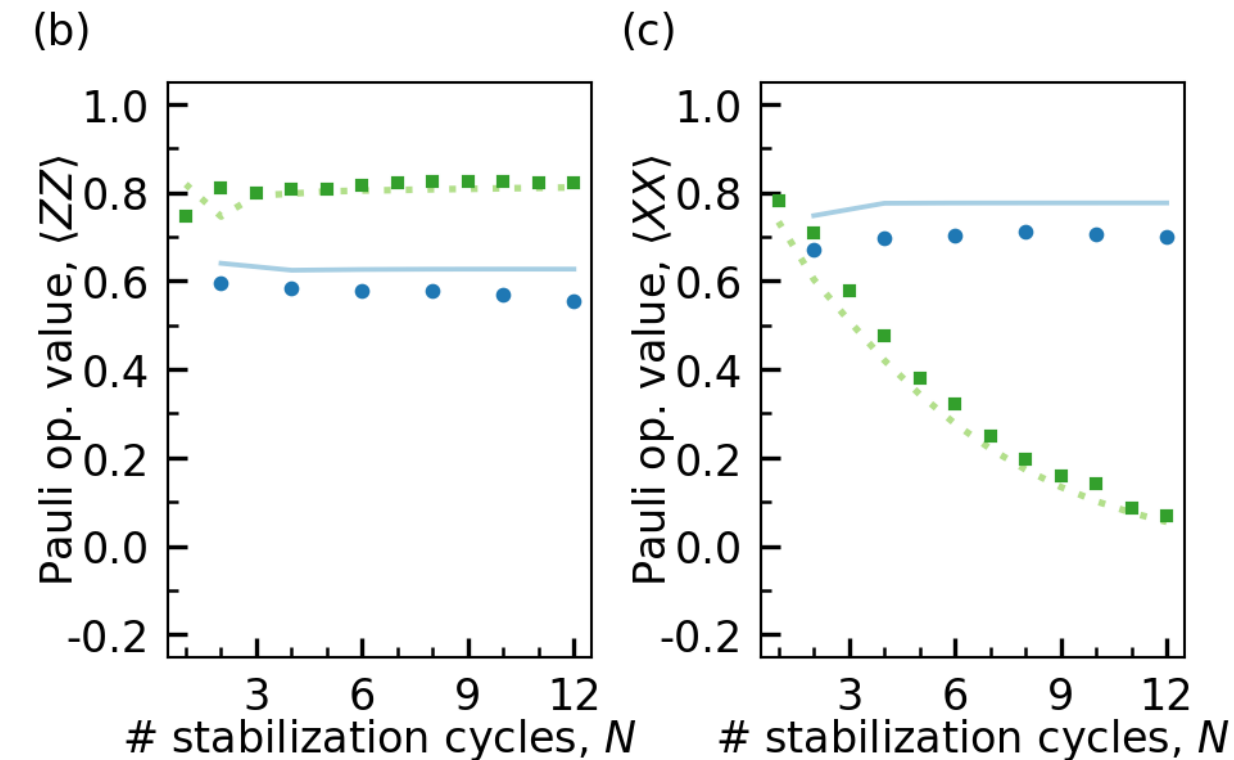
Fidelity:

- Experiment F = 74.5%
- Simulation F = 76.6%
- Overlap F = 95.5%

Repeated (6x) Weight-2 ZZ- & XX-Parity Msrmnts with Feedback



- Bell state fidelity decays when only repeating ZZ stabilization.
- Bell state fidelity is preserved for up to 18 us when stabilizing ZZ- & XX-parity.



- For only ZZ stabilization, $\langle XX \rangle$ decays as expected from simulations

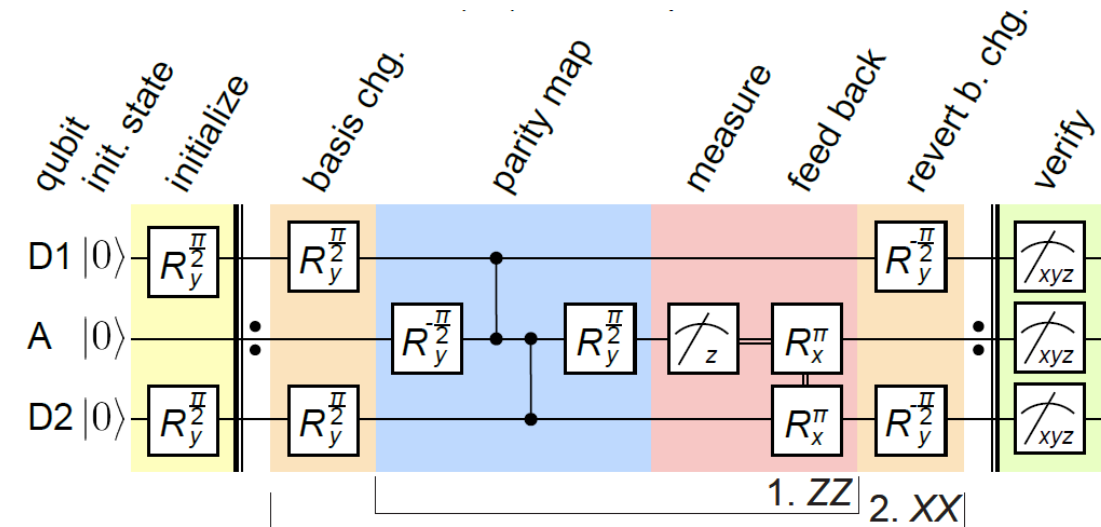
Entanglement Stabilization with Parity Measurements and Feedback

Results

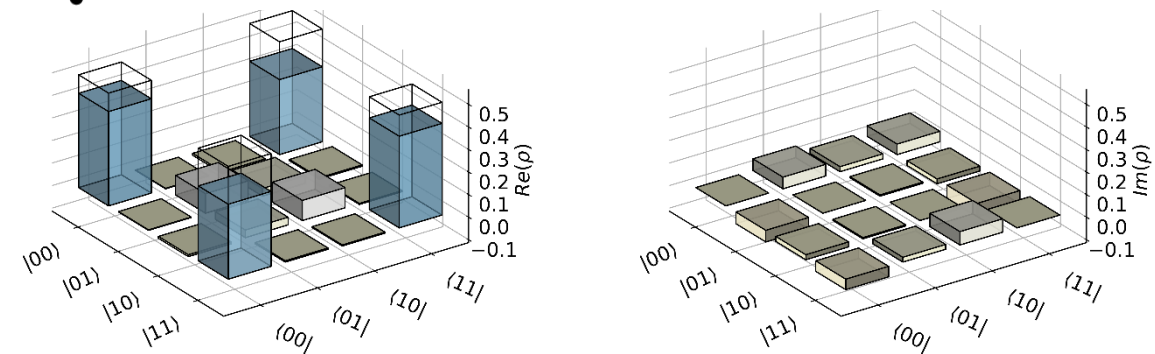
- Demonstrated weight-2 parity measurement of ZZ and XX.
- Bell state stabilized for 12 rounds of ZZ- & XX- parity stabilization with 74% fidelity.
- Realizes important element for future quantum error correction schemes.
- performance currently limited by feedback latency in relation to T_1 and T_2

Outlook

- Extend toward surface code
- Next step: weight-4 parity checks with feedback
- Surface 7 and Surface 17 codes



R_{xyz}^θ single qubit gate
 f_{xyz} measurement
 $\parallel : \parallel$ n repetitions
 \bullet two-qubit gate
 --- feedback



A Single Architecture ...

... for fast, high fidelity single shot readout

$F \sim 98.25$ (99.2) % at 48 (88) ns integration time and resonator population $n \sim 2.2$ with

- Optimized sample design
- Low-noise phase-sensitive Josephson parametric amplifier

T. Walter, P. Kurpiers *et al.*, *Phys. Rev. Applied* 7, 054020 (2017)

... for unconditional reset

- 99% reset fidelity in < 300 ns

P. Magnard *et al.*, *Phys. Rev. Lett.* 121, 060502 (2018)

... that is multiplexable

- Single feedline for 8 qubits (nodes)
- Reduced cross-talk using Purcell filters

J. Heinsoo *et al.*, *Phys. Rev. Applied* 10, 034040 (2018)

... for parity check with feedback and reset

C. Andersen, A. Remm, S. Balasius *et al.*, *arXiv:1902.06946* (2019)

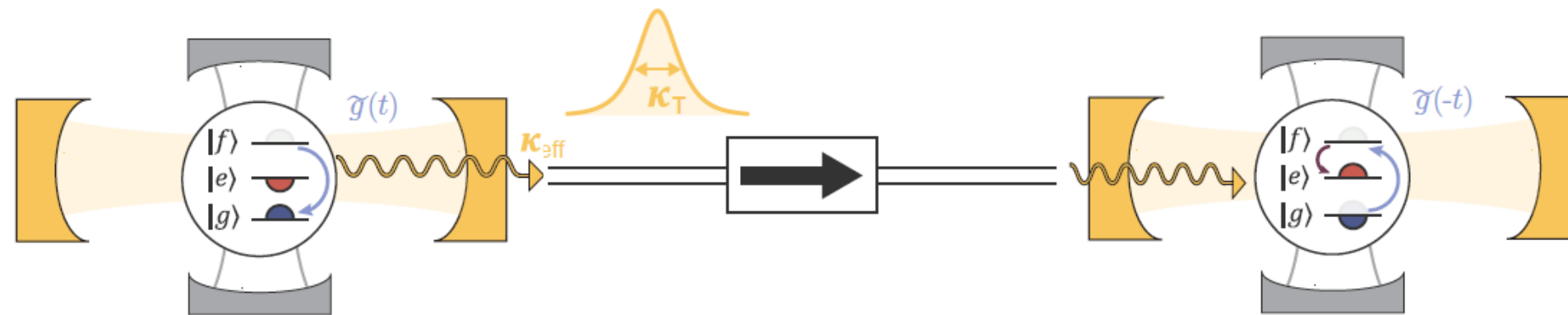
... for remote entanglement and state transfer, with time-bin encoding against photon loss

- Deterministic, 50 kHz rate
- ~ 80% transfer and entanglement fidelity

P. Kurpiers, P. Magnard *et al.*, *Nature* 558, 264 (2018)

P. Kurpiers, M. Pechal *et al.*, *arXiv:1811.07604* (2018)

Networks for Quantum Communication and Distributed Computing



Nodes of quantum network

- Store ...
 - Process ...
 - Send ...
 - Receive ...
- ... quantum information

A. Fowler et al., Phys. Rev. Lett., 104, 180503 (2010)

L.-M. Duan and C. Monroe, Rev. Mod. Phys. 82, 1209 (2010)

Reiserer and G. Rempe, Rev. Mod. Phys. 87, 1379 (2015)

Applications

- Expanding quantum processors by connecting modules
- Performing error correction across different nodes
- Generating distributed entanglement for communication using repeaters

Desired properties of channel

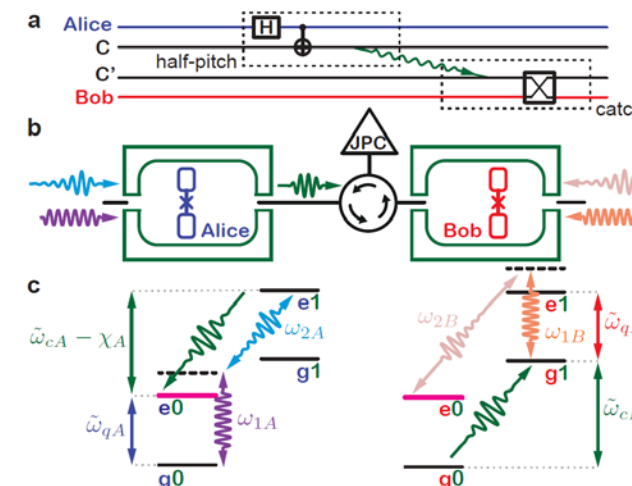
- Coherent
- Deterministic
- High data rate



Deterministic Remote Entanglement with Microwave Photons

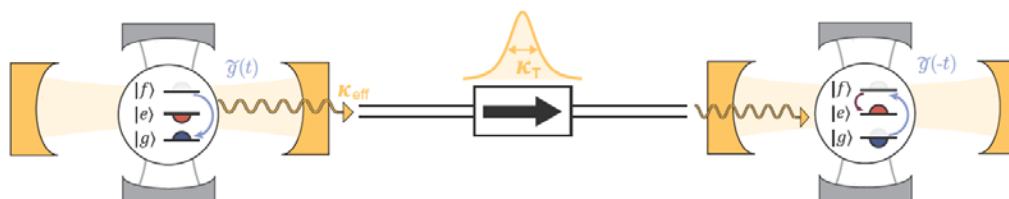
Mediated by Blue-Sideband: 3D

P. Campagne-Ibarcq *et al.*, *Phys. Rev. Lett.* 120, 200501 (2018)



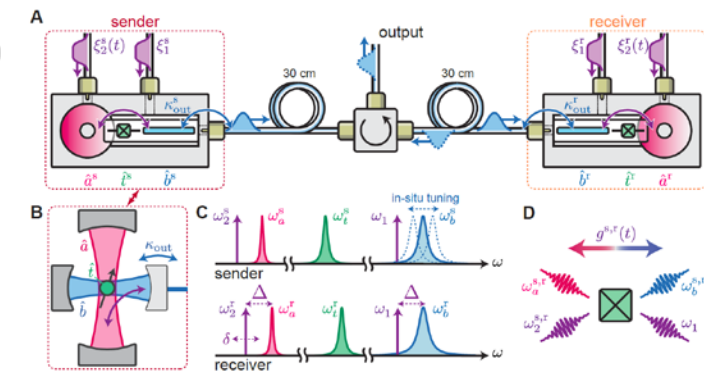
Mediated by Raman Process: 2D

P. Kurpiers, P. Magnard *et al.*, *Nature* 558, 264 (2018)



Mediated by Parametric Conversion: 3D

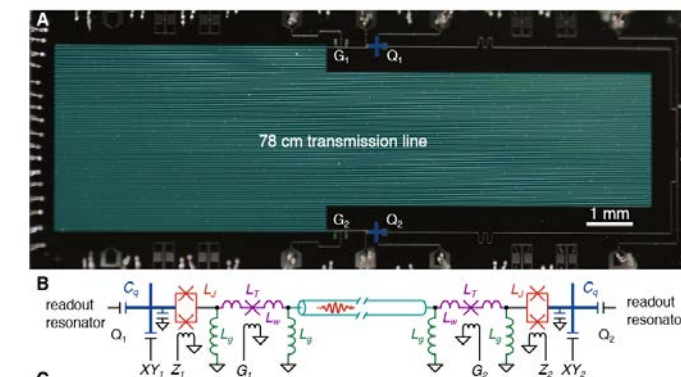
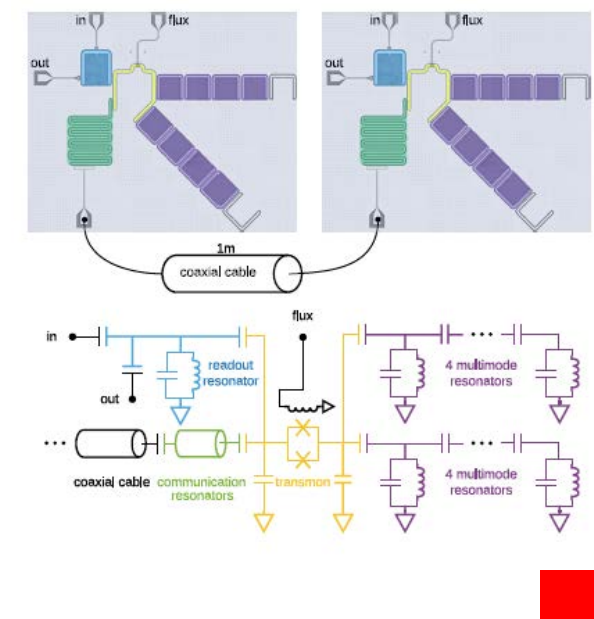
C. Axline *et al.*, *Nature Physics* 14, 705 (2018)



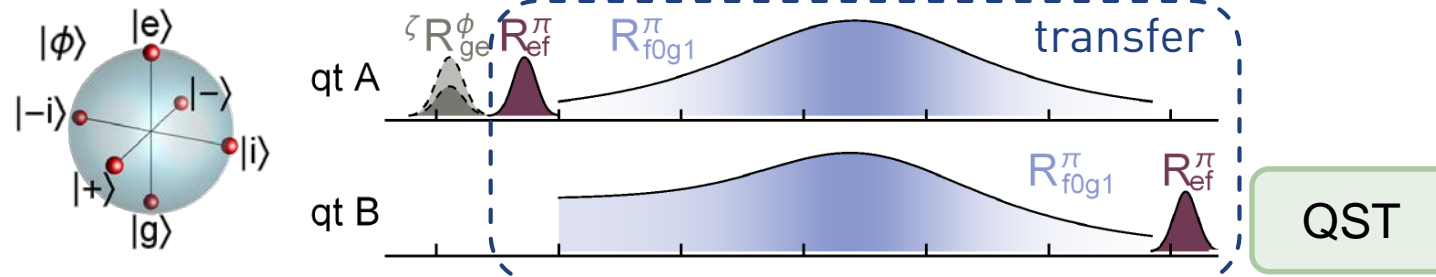
Mediated by Multimodal Channel with tunable coupling: 2D

N. Leung *et al.*, *arXiv:1804.02028* (2018)

Y. Zhong *et al.*, *arXiv:1808.03000* (2018)



Process Tomography of Quantum State Transfer



Input state:

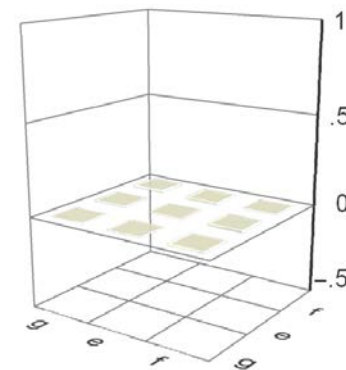
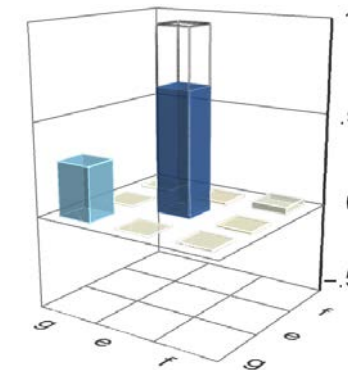
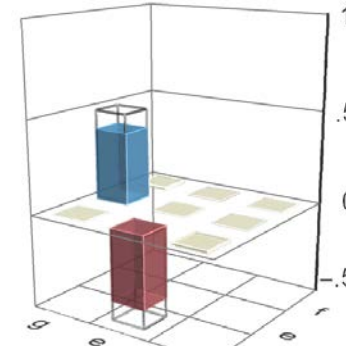
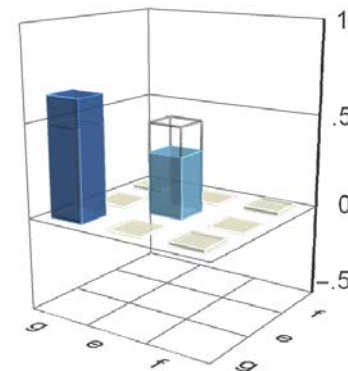
$$|i\rangle = \frac{1}{\sqrt{2}}(|g\rangle + i|e\rangle)$$

$$\mathcal{F}_{|i\rangle}^s = 87.9 \pm 0.1 \%$$

$|e\rangle$

$$\mathcal{F}_{|e\rangle}^s = 66.8 \pm 0.1 \%$$

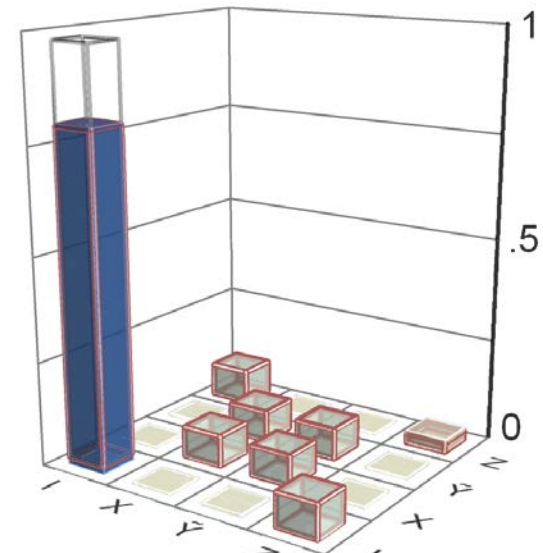
Output state:



- Prepare qubit A in six mutually unbiased input states $|\phi\rangle$
- Quantum state tomography on qubit B

QST

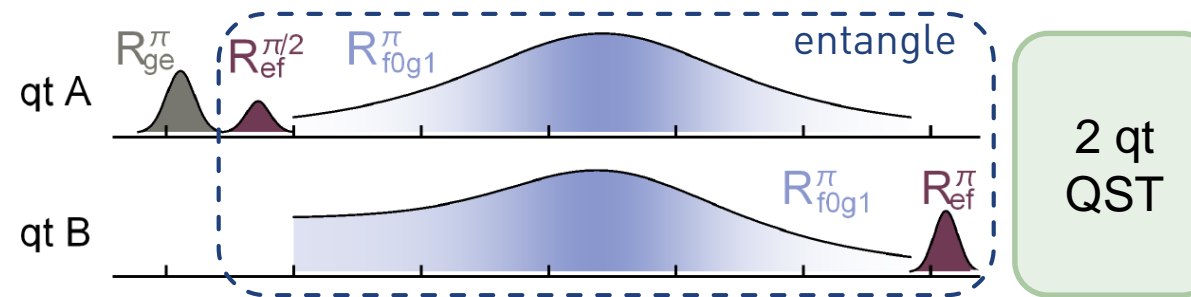
- Average state fidelity
- $\mathcal{F}_{\text{avg}}^s = \frac{1}{6} \sum \langle \phi | \rho_m | \phi \rangle = 86.0 \pm 0.1 \% > 2/3$



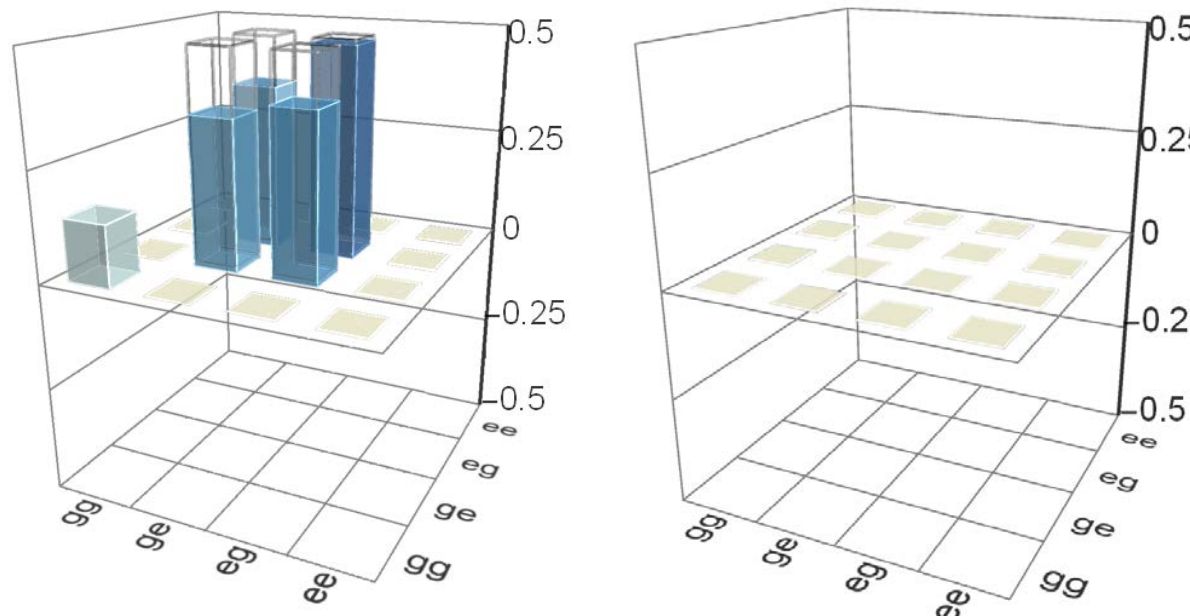
Transfer Process Matrix:

- Process fidelity
- $\mathcal{F}^p = \text{Tr}(\chi \chi_{\text{ideal}}) = 80.02 \pm 0.07 \% > 1/2$
- trace distance from MES $\sqrt{\text{Tr}[(\chi_m - \chi_{\text{sim}})^2]} = 0.014$

Generation of Remote Entanglement



Density matrix of qubit pair:



Protocol:

- Use entanglement scheme
- Perform full 2-qutrit state tomography

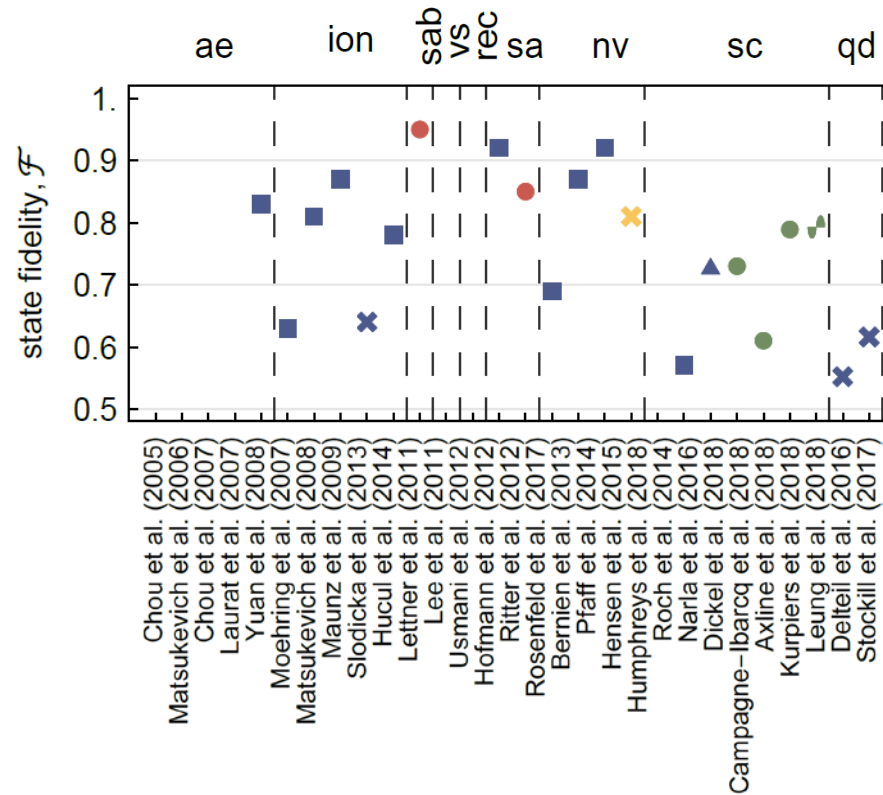
2-qubit subspace of 2-qutrit system

- Bell-state $|\psi^+\rangle = (|e, g\rangle + |g, e\rangle)/\sqrt{2}$
- Fidelity $\mathcal{F}_{avg}^s = \langle \psi^+ | \rho_m | \psi^+ \rangle = 78.9 \pm 0.1 \%$
- Concurrence $\mathcal{C}(\rho_m) = 0.747 \pm 0.004$

Master Equation Simulation:

- Infidelity: $1 - \mathcal{F}_{avg}^s = 21.1 \%$ from
 - $\sim 10.5 \%$ photon loss
 - $\sim 9 \%$ finite transmon coherence times
 - $\sim 1.5 \%$ imperfect absorption or pulse truncation

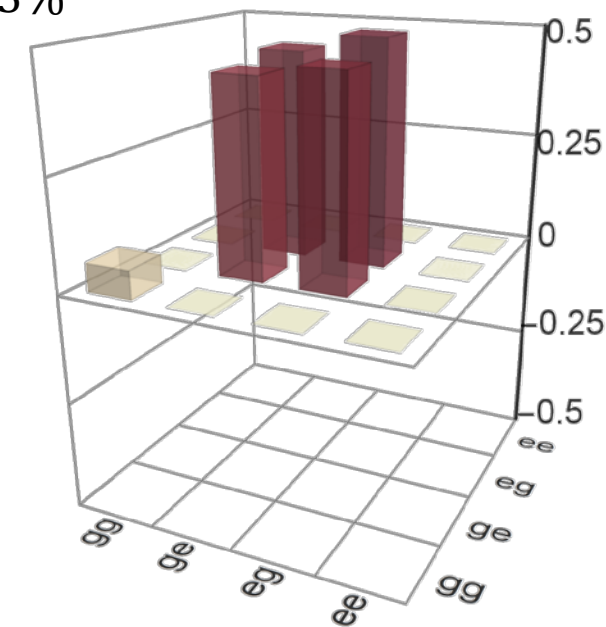
Performance Metric Summary and Next Steps



- state transfer rate: $\Gamma = 50\text{kHz}$
- concurrence of remote entanglement protocol:
 $C = 0.75$
- deterministic (un-heralded) remote entanglement fidelity: $F = 0.80$

Room for improvements (verified in simulations)

- With reduced photon loss and advances in qutrit coherence:
 - $\frac{\kappa}{2\pi} = 18 \text{ MHz}$, 12% photon loss, $T_1 = T_2 \sim 30 \mu\text{s}$
 - $\mathcal{F}_{sim} = \langle \psi^+ | \rho_{sim} | \psi^+ \rangle \sim 93\%$



- Further improvements expected by heralding
P. Kurpiers, M. Pechal *et al.*, *arXiv:1811.07604* (2018)

A Single Architecture ...

... for fast, high fidelity single shot readout

$F \sim 98.25$ (99.2) % at 48 (88) ns integration time and resonator population $n \sim 2.2$ with

- Optimized sample design
- Low-noise phase-sensitive Josephson parametric amplifier

T. Walter, P. Kurpiers *et al.*, *Phys. Rev. Applied* 7, 054020 (2017)

... for unconditional reset

- 99% reset fidelity in < 300 ns

P. Magnard *et al.*, *Phys. Rev. Lett.* 121, 060502 (2018)

... that is multiplexable

- Single feedline for 8 qubits (nodes)
- Reduced cross-talk using Purcell filters

J. Heinsoo *et al.*, *Phys. Rev. Applied* 10, 034040 (2018)

... for parity check with feedback and reset

C. Andersen, A. Remm, S. Balasius *et al.*, *arXiv:1902.06946* (2019)

... for remote entanglement and state transfer, with time-bin encoding against photon loss

- Deterministic, 50 kHz rate
- ~ 80% transfer and entanglement fidelity

P. Kurpiers, P. Magnard *et al.*, *Nature* 558, 264 (2018)

P. Kurpiers, M. Pechal *et al.*, *arXiv:1811.07604* (2018)

... for QND single-shot single photon detection

- 71% internal detection fidelity
 - 13% dark count probability
 - 16% detection inefficiency

J.-C. Besse *et al.*, *Phys. Rev. X* 8, 021003 (2018)

The ETH Zurich Quantum Device Lab

incl. undergrad and summer students



Challenges and Open Questions ...

... scaling and coherence: Increasing circuit complexity (scaling) while enhancing device coherence

- 3D integration
- Low loss materials
- Surface passivation

... tunable couplings and improved gates:

- 2-qubit gates with large on/off ratios
- Reduced cross-talk

... targeted error correction schemes

- Target implementation specific error syndromes
- Leakage detection

... viable NISQ era applications: realistic requirements for

- Quantum chemistry
- Drug design
- Optimization

... new collaboration models: Is a quantum CERN needed?

- Publicly funded long-term program (10-20 years)
- Long-term research and development staff
- Developing engineering expertise

... education

- Quantum engineering